$N^4C-Alkyl-N^4C$ Cross-Linked DNA: Bending Deformations in Duplexes that Contain a −CNG− Interstrand Cross-Link†

Anne M. Noronha, Christopher J. Wilds, and Paul S. Miller*

Department of Biochemistry and Molecular Biology, Bloomberg School of Public Health, Johns Hopkins University, 615 North Wolfe Street, Baltimore, Maryland 21205

Received February 12, 2002

ABSTRACT: Short DNA duplexes containing a 1,3-$N^4C-alkyl-N^4C$ interstrand cross-link that joins the two C residues of a −CNG− sequence were prepared using either a phosphoramidite or convertible nucleoside approach. The alkyl cross-link consists of 2, 4, or 7 methylene groups. The duplexes, which contain a seven-base-pair core and A_3/T_3 complementary 3′-overhanging ends, were characterized by enzymatic digestion and MALDI-TOF mass spectrometry. Ultraviolet thermal denaturation studies showed that the duplexes denature in a cooperative manner and that the length of the cross-link affects the thermal stability. Thus, the transition temperature of the ethyl cross-linked duplex, 42 °C, is 16 °C higher than the melting temperature of the corresponding non-cross-linked control, whereas the transition temperatures of the butyl and heptyl cross-linked duplexes, 73 and 72 °C, respectively, are 46−47 °C higher. The reduced molecularity of denaturation of the cross-linked duplexes versus melting of the non-cross-linked duplex most likely accounts for these differences. Examination of molecular models suggests that the ethyl cross-link is too short to span the distance between the two C residues at the site of the cross-link in B-form DNA without causing distortion of the helix, whereas less and no distortion would be expected for the butyl and heptyl cross-links, respectively. The circular dichroism spectra, which show greatest deviation in the ethyl cross-linked duplex from B-form DNA, are consistent with this expectation. Anomalous mobilities on native polyacrylamide gels of multimers produced by self-ligation of each of the cross-linked duplexes suggest that the ethyl and butyl cross-linked duplexes undergo bending deformations, whereas multimers derived from the heptyl cross-linked duplex migrated normally. The bending angle was estimated to be 20°, 13°, and 0° for the ethyl, butyl, and heptyl cross-linked duplexes, respectively. Thus, it appears that the degree of bending in these $N^4C-alkyl-N^4C$ cross-linked duplexes is controlled by the length of the cross-link.

Many clinically important cancer chemotherapeutic agents react with DNA to produce interstrand cross-links (*1*). These lesions are potentially lethal because they can inhibit both DNA transcription and replication (*2*−*4*). There has been considerable interest in studying how interstrand cross-links affect the structure of DNA and how interstrand cross-links are repaired by cells.

A variety of bifunctional alkylating agents, nitrogen mustards in particular, react with −GNC− sequences in DNA to produce 1,3-$N^7G-alkyl-N^7G$ interstrand cross-links. Short DNA duplexes that contain such cross-links have been synthesized and these duplexes have provided substrates for repair studies (*5*, *6*) and studies of the physical properties of the duplexes (*7*, *8*). However, the inherent chemical instability of $N^7G-alkyl-N^7G$ interstrand cross-links makes such duplexes difficult to work with, and this places some limitations on the types of studies that can be carried out.

We recently described the syntheses and physical properties of short DNA duplexes that contain $N^4C-ethyl-N^4C$ interstrand cross-links (*9*−*11*). The $N^4C-ethyl-N^4C$ cross-link is very stable chemically, and DNA duplexes containing this cross-link are readily synthesized on an automated DNA synthesizer in quantities sufficient for a variety of physical and biochemical studies. Although such cross-links are not found as products of DNA alkylation, they can serve as useful and easily manipulated models of DNA having alkyl interstrand cross-links. In addition, the chemistry allows one to place the cross-link in a variety of orientations. Thus, we have prepared duplexes that contain the interstrand cross-link between two mismatched C−C residues and duplexes having staggered cross-links in which the C residues of a −CG− or −GC− step are joined (*11*). It is clear from these studies that the orientation of the cross-link significantly affects the thermal stability and the structure of the duplex.

In the present studies, we describe the syntheses and conformational properties of short DNA duplexes that contain 1,3-$N^4C-alkyl-N^4C$ interstrand cross-links. This cross-link, which contains 2, 4, or 7 methylene groups, joins the C residues of a −CNG− sequence in the duplex. Ultraviolet thermal denaturation experiments show that the length of the cross-link influences the thermal stability of the duplex. Electrophoretic mobility shift experiments suggest that the cross-link introduces bending deformations in the helix and

† This research was supported by a grant from the National Cancer Institute (CA082785). A.M.N. and C.J.W. were each supported in part by postdoctoral fellowships from the Natural Sciences and Engineering Research Council of Canada (NSERC).

* Corresponding Author. Phone: 410-955-3489. Fax: 410-955-2926. E-mail: pmiller@jhsph.edu

10.1021/bi025671j CCC: $22.00
Published on Web 06/14/2002

that the degree of bending is controlled by the length of the cross-link.

MATERIALS AND METHODS

5′-O-Dimethoxytrityl-3′-O-(β-cyanoethyl-N,N′-diisopropyl)phosphoramidites, 3′-O-dimethoxytrityldeoxyribonucleoside-5′-O-(β-cyanoethyl-N,N′-diisopropyl)phosphoramidites, and protected deoxyribonucleoside-controlled pore glass supports were purchased from Glen Research Inc, Sterling, VA, or ChemGenes Inc, Ashland, MA. 5′-O-Dimethoxytrityl-3′-O-*tert*-butyldimethylsilyl-4-(N-1-triazole)-2′-deoxyuridine (*9*) and 1-[N^4-(5′-O-dimethoxytrityl-3′−O-*tert*-butyldimethylsilyl-2′-deoxycytidylyl)]-2-[N^4-(5′-O-dimethoxytrityl-2′-deoxycytidylyl-3′-O-(β-cyanoethyl-N,N′-diisopropyl)phosphoramidite)]ethane (*11*), **3**, were prepared as described previously. Oligonucleotide syntheses were carried out on an ABI Model 392 DNA synthesizer.

Analytical reversed-phase HPLC was carried out on a Microsorb-C-18 column (0.46 X 15 cm) purchased from Varian Associates, Walnut Creek, CA. The column was eluted at a flow rate of 1.0 mL/min with a 20 mL linear gradient of 2−20% acetonitrile in 50 mM sodium phosphate buffer, pH 5.8. Analytical and preparative strong anion exchange (SAX) HPLC was carried out on a Dionex DNAPAC PA-100 column (0.4 cm × 25 cm) purchased from Dionex Corp., Sunnyvale, CA. The column was eluted at a flow rate of 1.0 mL/min with a 30 mL linear gradient of 0.0 M to 0.5 M sodium chloride in a buffer containing 100 mM Tris-hydrochloric acid, pH 7.8, and 10% acetonitrile. The column was monitored at 260 nm (analytical runs) or 290 nm (preparative runs).

Polyacrylamide gel electrophoresis (PAGE) was carried out under denaturing conditions on 20 cm × 20 cm × 0.75 cm gels containing 20% acrylamide and 7 M urea in a buffer (TBE) that contained 89 mM Tris, 89 mM boric acid, and 0.2 mM ethylenediaminetetraacetate, pH 8.0. Native PAGE was carried out on 20 cm × 40 cm × 0.75 cm gels that contained 12% polyacrylamide in TBE. [^{32}P]-Labeled oligonucleotides were detected by autoradiography or by phosphorimaging.

Mass spectra were obtained at the Johns Hopkins University School of Medicine Mass Spectrometry Facility or at the Scripps Research Institute Mass Spectrometry Facility.

5′-O-Dimethoxytrityl-3′-O-tert-butyldimethylsilyl-4-N^4-(2-aminobutyl)-2′-deoxycytidine (4, n = 4). 5′-O-Dimethoxytrityl-3′-O-*tert*-butyldimethylsilyl-4-(N-1-triazole)-2′-deoxyuridine nucleoside (2.0 g, 2.87 mmol) was dissolved in 1,4-dioxane (29 mL). 1,4- Diaminobutane (0.727 mL, 7.18 mmol) was added slowly, and the reaction solution was stirred at room temperature for 1 h. The solvent was then evaporated to a syrup under high vacuum. The gum was redissolved in ethyl acetate (100 mL) and extracted with 5% sodium bicarbonate (2 × 100 mL); the excess amine appeared in the aqueous layer, as identified on ninhydrin-treated TLC plates as a white spot at the baseline on a lavender-colored background. The organic layer was dried over anhydrous sodium sulfate and then concentrated to a light yellow foam (1.01 g). UV max in methanol, 233 and 275 nm. R_f (SiO_2): 0.24 in methylene chloride/methanol, 8:2 (v/v). ESI MS calcd. 714.38, found MH^+ 715. Several milligrams of the product were treated with 0.1N hydrochloric acid for 1 h at 65 °C and analyzed by reversed-phase HPLC. The product, N^4−(4-aminobutyl)−2′-deoxycytidine, eluted at 8.2 min.

Scheme 1: Preparation of Cross-Linked Duplexes[a]

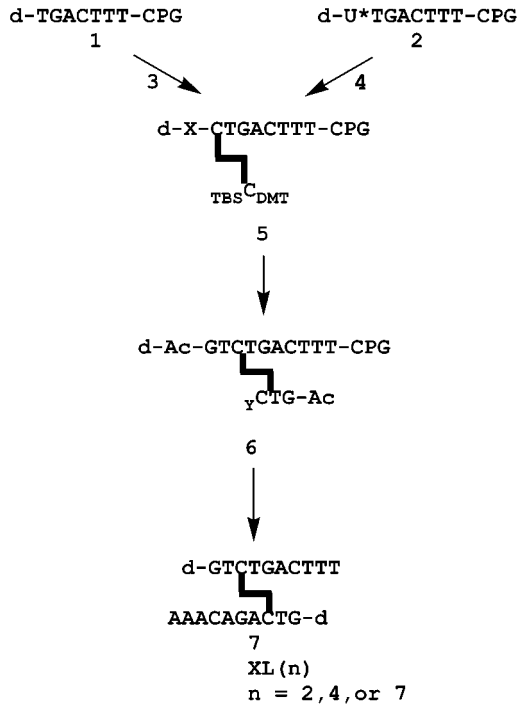

[a] U* is O^4−triazole−2′-deoxyuridine.

5′-O-Dimethoxytrityl − 3′-O-tert-butyldimethylsilyl-4-N^4-(2-aminoheptyl)-2′-deoxycytidine (4, n = 7). 5′-O-Dimethoxytrityl-3′-O-*tert*-butyldimethylsilyl-4-(N-1-triazole)-2′-deoxyuridine nucleoside (1.8 g, 2.5 mmol) was dissolved in 1,4-dioxane (25 mL) and reacted with 1,7-diaminoheptane (1.2 mL, 8.25 mmol) as described above. After workup and extraction, the organic layer was dried over anhydrous sodium sulfate and then concentrated to a light yellow foam (1.7 g). UV max in methanol, 233 and 275 nm. R_f (SiO_2): 0.26 in methylene chloride/methanol, 9:1 (v/v); 0.57 in toluene/ethyl acetate/methanol, 4.5/4.5/1.0 (v/v/v). ESI MS calcd. M 756.43, found MH 757.

Several milligrams of the product were treated with 0.1N hydrochloric acid for 1 h at 65 °C and analyzed by reversed-phase HPLC. The product, N^4−(7-aminoheptyl)−2′-deoxycytidine, eluted at 15.5 min.

Syntheses of Cross-Linked Duplexes. The cross-linked duplexes were prepared as outlined in Scheme 1 and as described previously (*9*, *11*). For duplexes containing the N^4C−ethyl−N^4C cross-link, 2 μmol of support bound heptamer, **1**, was reacted with 0.15 M cross-link phosphoramidite **3** for 10 min on the DNA synthesizer to give oligomer **5** (X = DMT). Duplexes containing either the N^4C−butyl− or heptyl−N^4C cross-link were prepared by reacting 2 μmol of support-bound octamer, **2**, which has a 5′-terminal O^4−triazole−deoxyuridine, with 21 mg (0.029 mmol) of **4** (*n* = 4) or 23 mg (0.030 mmol) of **4** (*n* = 7) in 100 μL of dry pyridine for 100 hrs at 45 °C. These reactions were carried out in a 4 mL autosampler vial fitted with a Teflon-lined screw top (Fisher Scientific). At the end of the reaction, the controlled pore glass was transferred back to the ABI synthesis column, and the support, **5** (X = OH), was washed with two, 10 mL portions of acetonitrile. The 5′-ends of **5** were extended simultaneously using 0.15 M

Table 1: Amounts, Retention Times, Nucleoside Ratios, and Mass Spectral Data for Cross-Linked Duplexes

cross-linked duplexes	amount[a]	R_t[b]	nucleoside composition	nucleoside ratios		mass	
				expected	observed	expected	observed
XL(2)	16.0 (164)	25.0	dC	1.00	1.00	6079.1	6079.5
			dG	2.00	2.04		
			dT	3.00	2.87		
			dA	3.00	2.96		
			dC-dC	0.50	0.73		
XL(4)	3.4 (20)	24.1	dC	1.00	1.00	6107.2	6108.2
			dG	2.00	2.04		
			dT	3.00	3.07		
			dA	3.00	2.75		
			dC-dC	0.50	0.52		
XL(7)	3.0 (20)	23.9	dC	1.00	1.00	6149.3	6149.5
			dG	2.00	1.96		
			dT	3.00	2.94		
			dA	3.00	2.68		
			dC-dC	0.50	0.53		

[a] Amount of pure cross-linked duplex that was purified by SAX HPLC. The numbers in parentheses indicate the amount of crude duplex that was purified. [b] Retention times (min) of cross-linked duplexes on SAX HPLC using a 0.0−0.5 M linear gradient of sodium chloride.

solutions of protected nucleoside−3′-phosphoramidites and a coupling time of 2 min. The synthesizer was programmed to acetylate the 5′-ends of the partial duplex after removal of the last DMT groups to give **6** (Y = TBS). The support was treated with 1 mL of anhydrous triethylamine at room temperature for 16 h. The support was washed with dry acetonitrile, followed by dry THF, and then dried under vacuum; It was then treated with 1 mL of 1 M solution of tetra-*n*-butylammonium fluoride in tetrahydrofuran for 20 min at room temperature. This solution had been stored previously over 4 Å molecular sieves. Synthesis was continued on 1 μmol portions of each support. The 3′-end of partial duplex **6** (Y = OH) was extended by reaction with 0.3 M solutions of the appropriate protected nucleoside−5′-phosphoramidites for 2 min.

The protecting groups were removed from each duplex by treating the support with 0.4 mL of concentrated ammonium hydroxide for 4 h at 65 °C. Between 82 and 164 A_{260} units of each duplex were obtained. Portions of each cross-linked duplex, **7**, were analyzed and purified by SAX HPLC as shown in Figure 2. The purified duplexes were desalted using C-18 reversed-phase SEP PAK cartridges as described previously (*9*). Each duplex migrated as a single band on a denaturing 20% polyacrylamide gel after phosphorylation with γ-[^{32}P]-ATP catalyzed by polynucleotide kinase (*9*).

The duplexes were digested to their component nucleosides and cross-link by treatment with a combination of snake venom phosphodiesterase and alkaline phosphatase (*9*). The digests were analyzed by C-18 reversed-phase HPLC, and the nucleoside ratios were determined as shown in Table 1. Nucleoside ratios obtained by this procedure are generally within ±0.1 of the expected values. The duplexes were further characterized by MALDI TOF mass spectrometry. The results are given in Table 1.

Circular Dichroism Spectroscopy. Solutions of each cross-linked duplex, 2 μM strand, and the control non-cross-linked duplex, **C(0)**, 3.6 μM strand, were prepared in a buffer containing 90 mM sodium chloride, 10 mM sodium phosphate, 1 mM EDTA, pH 7.0. The samples were equilibrated for 5−10 min at 5 °C, and their CD spectra were recorded on a Jasco J-700 spectropolarimeter equipped with a NESLAB RTE−111 circulating bath. Spectra were collected at a rate of 100 nm/min with a bandwidth of 1 nm and sampling wavelength of 0.2 nm using fused quartz cells (Hellma, 165-QS). The molar ellipticity was calculated from the equation $[\theta] = \theta/Cl$, where θ is the relative ellipticity (mdeg), C is the concentration of the oligonucleotide (mol/L) and l is the path length of the cell (cm). The data were processed on a PC computer using software supplied by the manufacturer. Each spectrum shown in Figure 3 is the average of 5 scans.

Thermal Denaturation Experiments. Solutions, 1 μM each strand, of each cross-linked duplex and of the control non-cross-linked duplex, **C(0)**, were prepared in a buffer containing 90 mM sodium chloride, 10 mM sodium phosphate, 1 mM EDTA, pH 7.0. The molar extinction coefficients of the oligonucleotides and cross-linked duplexes were calculated using nearest-neighbor approximations (*12*). Thermal denaturation experiments were run in a Cary 3E UV−vis spectrophotometer fitted with a thermostated sample holder and temperature controller. The absorbance at 260 nm was monitored as the samples were heated from 5 to 90 °C at a rate of 0.4 °C/min. Denaturation curves were generated by plotting the relative hypochromicity, defined as $(a_t - a_{5°C})/(a_{90°C})$, where a_t is the absorbance at temperature t, $a_{5°C}$ is the absorbance at the initial temperature of 5 °C, and $a_{90°C}$ is the absorbance at the final temperature of 90 °C, versus temperature.

Ligation Experiments. Cross-linked duplexes **XL(2)**, **XL(4)**, and **XL(7)**, a non-cross-linked control duplex, **C(0)**, of the same sequence, and duplex **M1**, d-GGGCAAAAAACG-GCAAAAAAC/d-CCGTTTTTTGCCGTTTTTTGC (*13*) (210 pmol), were each phosphorylated with γ-[^{32}P]-ATP in the presence of polynucleotide kinase as described previously (*9*). The enzyme was inactivated by heating at 65 °C for 10 min. A 50 pmol aliquot of each duplex was incubated with 5 units of T4 DNA ligase in a buffer that contained 50 mM Tris, pH 7.5, 10 mM magnesium chloride, 100 mM sodium chloride, 10 mM dithiothreitol, 1 mM ATP, and 25 μg/mL of bovine serum albumin. Reactions containing **XL(7)** or **C(0)** were incubated for 5 min at room temperature, whereas reactions containing **XL(2)**, **XL(4)** or **M1** were incubated overnight at 16 °C. A 2 μL aliquot of each reaction was diluted with 2 μL of 80% glycerol, and the solution was loaded onto a 12% polyacrylamide gel. The gel was run at

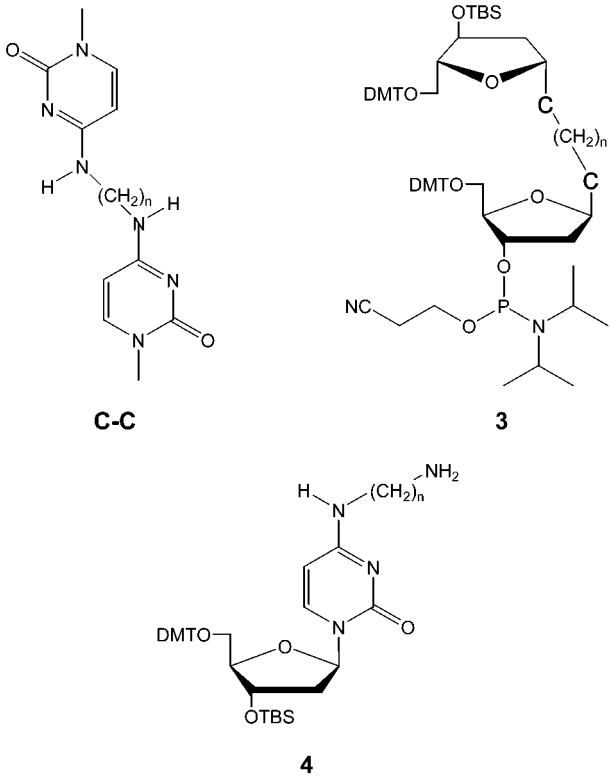

FIGURE 1: Structures of the N^4C−alkyl−N^4C interstrand cross-link (C−C), protected N^4C−alkyl−N^4C cross-link phosphoramidite (**3**), and protected N^4−(aminoalkyl)−2′-deoxycytidine (**4**).

650 V for approximately 5 h at 4 °C and then autoradiographed. The distances that the ligated cross-linked oligomers migrated were measured and compared to the distances migrated by oligomers produced by ligation of the non-cross-linked control duplex, **C(0)**.

Molecular Models. Molecular models of an 11-mer duplex, d-CCGGTCTGACC/d-GGTCAGACCGG, containing N^4C−alkyl−N^4C interstrand cross-links were built using Hyper Chem molecular modeling software. The cross-linked duplexes were geometry optimized using the AMBER force field. For ease of visualization, nucleotides on either side of the cross-link were removed as shown in Figure 7.

RESULTS

Syntheses of Cross-Linked Duplexes. The general structure of the interstrand cross-linked duplexes, **7**, is shown in Scheme 1 and the structure of the N^4C−alkyl−N^4C cross-link, **1**, is shown in Figure 1. The cross-link joins the two deoxycytidine residues on opposite strands of a −CTG−/−GAC− sequence. The duplexes are designated as **XL(n)**, where **(n)** indicates the length of the N^4C−alkyl−N^4C cross-link. A control duplex, **C(0)**, was also prepared that lacks the cross-link.

The cross-linked duplexes were prepared on a DNA synthesizer as shown in Scheme 1. Each synthesis was initially carried out on a 2 μmol scale. Two methods were used to introduce the cross-links. In the first method, protected N^4C−ethyl−N^4C phosphoramidite **3** (*11*), whose structure is shown in Figure 1, was coupled to support-bound heptamer **1** to give octamer **5** (X = DMT) which contains the cross-link. Alternatively, octamer **5** (X = 5′-OH) was prepared by reacting O^4−triazol−U-derivatized oligomer **2** with protected N^4−(4-aminobutyl)− or N^4−(7-aminoheptyl)−2′-deoxycytidine **4**. We have previously used this convertible nucleoside approach to prepare N^4C−ethyl−N^4C cross-linked duplexes (*9*). Approximately 77% of **2** was converted to **5** when reacted with the aminobutyl derivative of C. Similar extents of conversion were seen previously for reaction with the aminoethyl derivative of C (*9*). In contrast, only 54% of **2** was converted to **5** when the reaction was carried out using the aminoheptyl derivative of C.

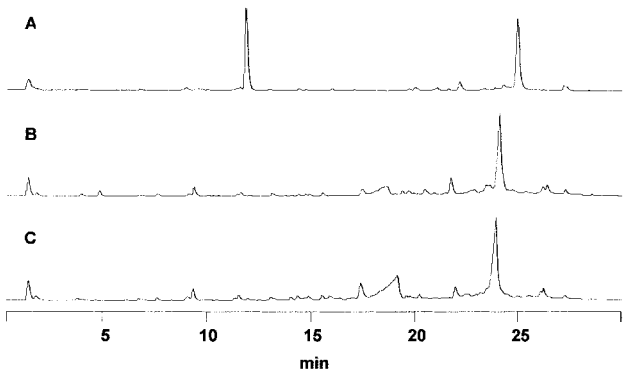

FIGURE 2: Strong anion exchange HPLC profiles of crude **XL(2)** (panel A), **XL(4)** (panel B), and **XL(7)** (panel C). The column, which was monitored at 260 nm, was eluted with a gradient of 0.0−0.5 M sodium chloride in 100 mM Tris-HCl, pH 7.8, 10% acetonitrile, at a flow rate of 1.0 mL/min.

The dimethoxytrityl group(s) were removed from cross-link derivatized oligomer **5**, and each 5′-end of the cross-link was extended in the 5′-direction to give, after acetylation of the 5′-hydroxyl groups, branched oligomer **6** (Y = TBS). Because both 5′ ends are extended simultaneously, only symmetrical sequences can be synthesized by this method. Oligomer **6** was treated with anhydrous triethylamine to remove the cyanoethyl phosphate protecting groups, a step that is required to prevent unwanted chain cleavage during subsequent removal of the *tert*-butyldimethylsilyl (TBS) group (*9*, *14*−*16*). The TBS group was removed from **6** by treating with 1 M tetra-*n*-butylammonium fluoride. Approximately 84% of the TBS group was removed from the N^4C−ethyl−N^4C cross-linked oligomer, whereas virtually quantitative removal was observed for the N^4C−butyl−N^4C and N^4C−heptyl−N^4C cross-linked oligomers.

The branched oligomer **6** (Y = 3′-OH) was extended in the 3′-direction by coupling with protected 3′-O-dimethoxytritylnucleoside-5′-O-phosphoramidites. The protecting groups were removed, and the oligomer was cleaved from the support by treating with concentrated ammonium hydroxide at elevated temperature. Figure 2 shows chromatograms of the crude cross-linked oligomers. The peak at 11.8 min in chromatogram A is D-TGACTTT, which resulted from a low coupling yield when using phosphoramidite **3**. The major side product observed in the synthesis of **XL(7)** was unextended branched oligomer **6** (Y═OH), whose retention time is 19.5 min, as shown in chromatogram C. Each cross-linked duplex was purified by preparative strong anion exchange HPLC. The duplexes were characterized by enzymatic digestion and by MALDI-TOF mass spectrometry, as shown in Table 1.

Circular Dichroism Studies. Circular dichroism (CD) spectra were obtained for each of the cross-linked duplexes and the non-cross linked control at 5 °C under the same

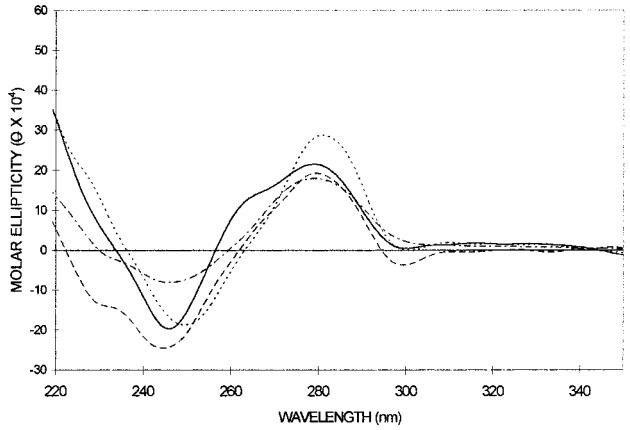

FIGURE 3: Circular dichroism spectra of **C(0)** (−·−), **XL(2)** (−), **XL(4)** (− − −), and **XL(7)** (···). Spectra were recorded at 5 °C in buffer containing 90 mM sodium chloride, 1 mM EDTA, 10 mM sodium phosphate, pH 7.0.

buffer conditions used in the thermal stability experiments. Under these conditions, the oligomers should be completely in the duplex form. The spectra are shown in Figure 3. The control duplex, **C(0)**, displays a spectrum consistent with that of B-form DNA with a maximum at 279 nm, a minimum at 246 nm, and a crossover at 259 nm. The CD spectra of **XL(4)** and **XL(7)** are similar, each having a relatively sharp positive band with maxima at 279 and 282 nm, respectively, and a slight shoulder at 263 nm. In contrast, **XL(2)** has a very broad positive band with a maximum at 279 nm and a very prominent shoulder at 262 nm. All three duplexes have a negative band whose minimum is between 245 and 251 nm. In addition, duplex **XL(4)** shows a small negative band at 300 nm. The molar ellipticities of the positive bands of **XL(2)** and **XL(4)** are similar to that of control duplex **C(0)**, whereas the molar ellipticity of **XL(7)** is 1.6 times greater than that of **C(0)**.

Thermal Stabilities of Cross-linked Duplexes. The thermal stabilities of the cross-linked duplexes were determined by UV melting experiments. In contrast to conventional duplexes, the very nature of the covalent cross-link precludes complete separation of the constituent strands. The denaturation curves are shown in Figure 4. The transition temperatures were concentration-independent, as expected for a unimolecular process.

Duplex **XL(2)** denatures in a cooperative manner, although the transition curve is rather broad. The transition temperature is 42 °C, which is higher than the melting temperature, 26 °C, of the non-cross-linked control duplex **C(0)**. Duplexes with the butyl and heptyl cross-links also show cooperative thermal denaturation. However, the breadths of these transitions are sharper and the transition temperatures are much higher than those of the corresponding ethyl cross-linked duplex. The transition temperature of **XL(4)** is 73 °C, while that of **XL(7)** is 72 °C.

Ligation Studies. The cross-linked duplexes and non-cross-linked control duplex were each 5′-end labeled with [^{32}P]-phosphate, and each duplex was then ligated at 16 °C using T4 DNA ligase. In addition, a 21-mer duplex, **M1**, that contains two −A_6− tracts (*13*) was ligated under the same conditions. The products of the ligation reactions were separated on a nondenaturing polyacrylamide gel as shown in Figure 5.

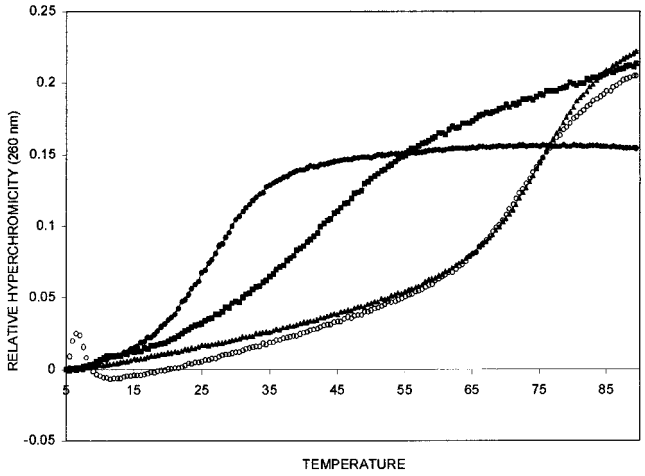

FIGURE 4: Thermal denaturation of **C(0)** (●), **XL(2)** (■), **XL(4)** (▲), and **XL(7)** (○). The denaturation curves were obtained in a buffer containing 90 mM sodium chloride, 1 mM EDTA, 10 mM sodium phosphate, pH 7.0.

The ligation products of control duplex **C(0)** yielded a series of oligonucleotides whose chain lengths differ by multiples of 10 base pairs, as shown in lane 2. Multimers generated by self-ligation of **M1** (lane 1) showed reduced mobility relative to the oligomers of the same chain length produced by self-ligation of **C(0)** (lane 2). Multimers generated from cross-linked duplexes **XL(2)** (lane 3) and **XL(4)** (lane 4) also showed reduced mobility, whereas multimers generated from **XL(7)** (lane 5) co-migrate with the control.

The relative lengths, R_L, of the ligation products from each duplex were determined by comparing their mobilities with those from the multimers produced by ligation of control duplex **C(0)** (*13*, *17*). These relative lengths were then plotted against the actual length of the multimers as shown in Figure 6. As expected, the ligation products of **M1** show a positive deviation from $R_L = 1.00$, consistent with bending induced by the presence of the −A_6− tracts in the oligomers (*13*). Cross-linked duplexes **XL(2)** and **XL(4)** also showed positive deviations. The deviation was greatest for **XL(2)**. In contrast to this behavior, duplex **XL(7)** gave essentially a straight line with an R_L of 1.00.

DISCUSSION

The −CNG− cross-linked duplexes described in these studies are in some respects similar to the 1,3-N^{7}G−alkyl−N^{7}G −GNC− type interstrand cross-links found when DNA reacts with bifunctional alkylating agents such as mechlorethamine (*7*) or phosphoramide mustard (*18*). Thus molecular models suggest that the alkyl chain of the cross-link resides in the major groove of the helix, and the N^4−alkyl−C residues can participate in Watson−Crick base pairing with their complementary G residues in the opposite strand.

The N^{4}C−alkyl−N^{4}C cross-link was introduced during synthesis of the duplex either as the protected phosphoramidite (*11*) or by a convertible nucleoside approach (*9*) as outlined in Scheme 1. Chain extension of cross-link intermediate **5** in the 5′-direction was carried out after selective removal of the dimethoxytrityl group(s) from **5**. Removal of the *tert*-butyldimethylsilyl group from the resulting branched **6** was affected by treating the support with a

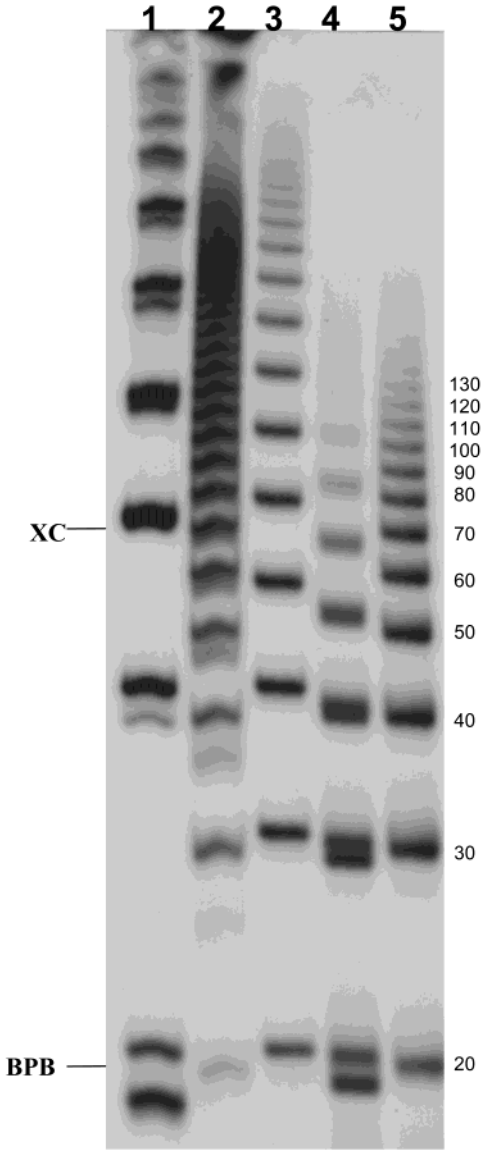

FIGURE 5: Self-ligation of cross-linked duplexes. 5′-Phosphorylated duplexes were ligated using T4 DNA ligase as described in Material and Methods. The ligation products of **M1** (lane 1), **C(0)** (lane 2), **XL(2)** (lane 3), **XL(4)** (lane 4), and **XL(7)** (lane 5) were subjected to electrophoresis on a 12% polyacrylamide gel run under non-denaturing conditions.

solution of tetra-*n*-butylammonium fluoride in dry tetrahydrofuran. We have found previously that removal of this group occurred with yields ranging from 50% to 70% (*9*, *11*). Higher desilylation yields, ranging from 84% for the ethyl-linked oligomer to essentially quantitative removal for the butyl- and heptyl-linked oligomers, were obtained with the present set of oligomers. These results support the previous suggestion that steric crowding in the neighborhood of the TBS group plays a important role in its accessibility to attack and removal by fluoride ion (*11*). Extension of **6** after removal of the TBS group with protected nucleoside 5′-phosphoramidites gave the completed cross-linked duplex **7**.

The cross-linked duplexes migrated as single peaks on strong anion HPLC and were readily purified by this method. The main side product seen in the syntheses of **XL(2)** was d-TGACTTT, whose retention time is 12.0 min (Figure 2A). This oligomer resulted from incomplete coupling of **1** with

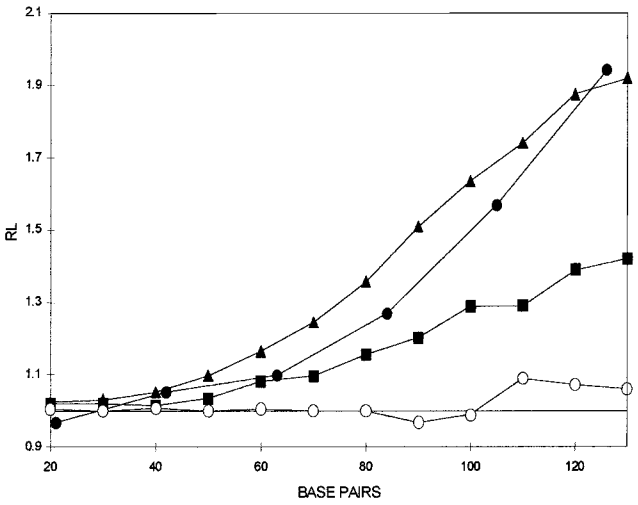

FIGURE 6: Relative chainlength (R_L) vs actual chainlength of the self-ligation products of **M1** (●), **XL(2)** (▲), **XL(4)** (■), and **XL-(7)** (○).

the N^4C−ethyl−N^4C phosphoramidite. The major side product in the syntheses of **XL(7)** was d-GTCTGACTTT, whose retention time is 19.1 min (Figure 2C). This oligomer resulted from incomplete reaction, 54%, of **2** with protected N^4−(7-aminoheptyl)−2′-deoxycytidine, **4**. The higher extents of conversion, seen with the N^4−(2-aminoethyl)− and N^4−(4-aminobutyl)−2′-deoxycytidines, 70−80% (*9*), most likely reflect the greater reactivity of the shorter aminoalkyl arms.

Each of the cross-linked duplexes can potentially form a helix containing 7 base pairs. The circular dichroism spectra of the three cross-linked duplexes, which are similar to that of canonical B-form DNA (*19*), are consistent with helix formation. Further evidence for helix formation comes from ultraviolet thermal denaturation experiments. Thus, each of the duplexes show A_{260} versus temperature profiles that are suggestive of cooperative denaturation. The duplex having the ethyl cross-link shows a broad, sigmoidal-shaped transition curve, which is much broader than the corresponding melting curve observed for the non-cross-linked control. However, the transition temperature for denaturation of the cross-linked duplex is 16 °C, higher than the melting temperature of the **C(0)**. This difference most likely reflects the reduced entropy due to the change in molecularity from second order for melting of **C(0)** to first order for denaturation of the cross-linked duplex (*20*).

Duplexes **XL(4)** and **XL(7),** in addition to having sharper transition curves, have transition temperatures that are 47 and 46 °C higher, respectively. than the melting temperature of **C(0)** and approximately 30 °C higher than the transition temperature of the ethyl cross-linked duplex, **XL(2)**. This large increase in stability is comparable to that seen previously for duplexes that contain a −CG− type N^4C−ethyl−N^4C cross-link (*11*).

The higher transition temperatures of the butyl and heptyl cross-linked duplexes relative to that of the ethyl cross-linked duplex, are consistent with the expected ability of these longer linkers to more readily span the distance between the two strands of the helix. Examination of molecular models shows the distance between the nitrogen atoms of the N^4-amino groups of the two interstrand C residues in a −CNG− sequence is approximately 7.2 Å when the helix is in the B-form conformation. The ethyl cross-link, which could

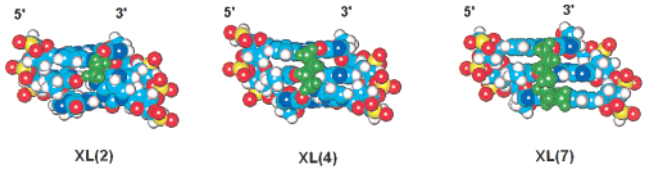

FIGURE 7: Molecular models of the −CNG− N^4C−alkyl−N^4C cross-link site. The ethyl (**XL(2)**), butyl (**XL(4)**), and heptyl (**XL(7)**) cross-links are shown in green.

maximally span 3.8 Å, is too short to span this distance. Geometry optimization of B-form DNA that contains the ethyl cross-link using the AMBER force field suggests considerable perturbation of the cross-linked C−G base pairs which could involve severe propeller twisting and displacement of the C residues into the major groove (see Figure 7). Such modeling cannot reliably predict more global conformational changes such as bending of the DNA helix. That structural perturbation does occur is reflected in the CD spectrum of **XL(2)**, which unlike the non-cross-linked control, shows a broad positive band and shoulder at 279 and 262 nm, respectively. These differences could result from changes in local stacking interactions of the bases at or near the site of the cross-link and/or a more global change in the geometry of the helix.

The butyl cross-link, which can maximally span a distance of 6.23 Å, would be expected to cause less perturbation to helix geometry. This is reflected in the geometry-optimized model of DNA containing this cross-link, which suggests that modest propeller twisting or rolling of the cross-linked C−G base pairs would result from insertion of the cross-link. Overall, the CD spectrum of **XL(4)** is consistent with that of B-form DNA, with the exception of the unusual small negative band at 300 nm, which suggests some perturbation of the helix geometry.

As shown in Figure 7, the geometry optimized model suggests that the heptyl cross-link is sufficiently long, 10.0 Å, to join the interstrand C residues without perturbing base pairing or base stacking interactions at the site of the cross-link. This expected lack of perturbation is reflected in the CD spectrum of **XL(7)**, which appears qualitatively quite similar to those of the control duplex **C(0)** and B-form DNA.

To further investigate the effects of the cross-links on helix geometry, each cross-linked duplex was self-ligated using T4 DNA ligase, and the products were analyzed by native polyacrylamide gel electrophoresis (*21*). All three cross-linked duplexes underwent self-ligation, although the kinetics of ligation were quite different. Non-cross-linked control **C-(0)** and cross-linked duplex **XL(7)** both generated substantial amounts of longer oligomers after 5 min incubation at 16 °C. In contrast, overnight incubation was required to generate long oligomers from ligation of **XL(2)**, **XL(4)** and $-A_6-$ tract containing a 21-mer, **M1**. Multimers produced by ligation of **XL(2)**, **XL(4),** or **XL(7)** have cross-links that are phased every 10 base pairs. The reduced electrophoretic mobilities of the multimers derived from **XL(2)** and **XL(4)** suggest that the ethyl and butyl cross-links produce an overall bending deformation in these molecules. In the case of **XL-(2)**, the degree of bending appears to be very similar to that produced by the $-A_6-$ tracts in duplex **M1**. Thus, a plot of R_L versus the size of the oligomer in base pairs gave a positively deflecting curve that is very similar to that seen for **M1**. A positively curved plot was also seen for the ligation products of butyl cross-linked **XL(4),** although in this case the magnitude of the curvature was approximately one-half that seen with **XL(2)** or **M1**. In contrast to this behavior, the plot of the ligation products of **XL(7)** did not deviate significantly from $R_L = 1.00$, suggesting that the heptyl cross-link does not produce bending deformations in the helix.

Multimers produced by ligation of the cross-linked duplexes will contain, in addition to the cross-links, $-A_3-$ tracts that are phased every 10 base pairs. Previous experiments by Nadeau and Crothers (*22*) suggest such tracts will not contribute to the bending deformations. To test this, the mobilities of the ligation products of **C(0)**, which also contain $-A_3-$ tracts phased every 10 base pairs, were compared to those generated by ligation of a *Bam* H1 linker, d-CGGGATCCCCG, a marker frequently used in bending experiments (*13*). The mobilities of the ligation products from **C(0)** and the *Bam* H1 linker were in fact identical (data not shown).

The cross-link induced deformation most likely results from static bending or anisotropic flexibility (*21*) and not from formation of a hinge joint (*17*) at the site of the cross-link. Thus, multimers produced from self-ligation of duplexes in which the cross-link is phased every 14 base pairs did not show anomalous electrophoretic mobilities (data not shown). As discussed by Rink and Hopkins (*8*), the presence of a hinge joint would be expected to produce anomalous mobilities independent of the phasing of the cross-link.

The bending angles of **XL(2)** and **XL(4)** were determined using the empirical relation developed by Koo and Crothers (*13, 17*):

$$C = \{[R_L - 1]/(9.6 \times 10^{-5})L^2 - 0.47\}^{1/2} \times (A_6) \quad (1)$$

where R_L is the relative length of the multimer, L is the actual length of the multimer, and A_6 is the absolute bending angle of an A_6 tract which has been determined to be approximately 20° (*13, 23*) Equation 1 was applied (*17*) to the 120 bp multimers of **XL(2)** and **XL(4)** to give bending angles of 20° and 13°, respectively. These angles may be compared to those of DNA duplexes containing other types of interstrand cross-links, including a transplatin G−C cross-link, 26° (*24*) or 20° (*25*), a cisplatin G−G cross-link, 55° (*26*) or 47° (*27*), and a mechlorethamine G−G cross-link, 12.4° − 16.8° (*8*).

It appears that the degree of bending is directly related to the length of the cross-link. This seems reasonable if the local, cross-link-induced distortions suggested by the geometry optimized models could be relieved by bending the helix toward the major groove. Thus, the shorter, ethyl cross-link would be expected to create greater bending than the butyl cross-link. Similar effects of linker length on bending were recently reported by Kowalczyk et. al. for a N^2G−alkyl−N^2G intramolecular cross-link connecting two adjacent G residues on one strand of a DNA duplex (*28*). In this case, the order of bending was two-carbon cross-link (∼30°) > three-carbon cross-link (12°) > four-carbon cross-link (7°).

No bending was observed for the duplex with the heptyl interstrand cross-link, **XL(7)**. Here the cross-link is of sufficient length to span the two C residues without introducing local perturbations. Similar lack of bending has been

observed in other cross-linked DNA duplexes. For example, no detectable bending was observed in duplexes that contained a mitomycin C (*29*) or a trimethylene (*30*) interstrand cross-link. Both of these cross-links reside in the minor groove of the helix. We have reported previously that DNA duplexes that contain a N^4C−ethyl−N^4C cross-link between mismatched C−C residues or the C residues in a −CG− step do not show anomalous electrophoretic mobilities. In these duplexes, the cross-links reside in the major groove of the helix. Examination of molecular models of the C−C mismatched cross-link suggests that the ethyl group can readily span the two C residues without perturbing the structure of the duplex. Similarly, the distance between the two C residues of the −CG− staggered cross-link is sufficiently short to be spanned by the ethyl cross-link. Thus, in both cases, it appears unlikely that the presence of the ethyl cross-links causes sufficient local structural perturbations that would give rise to overall bending deformations in the helix.

Our results with the −CNG− cross-linked duplexes suggest that it may be possible to control bending deformations by varying the length of the cross-link. DNA duplexes containing such cross-links might provide interesting substrates for studying the effects of DNA bending on interactions with nucleic acid binding proteins and proteins involved in DNA repair. High-resolution NMR studies are currently underway to better define the structure of these duplexes. In addition, we are investigating their repair in prokaryotic and eukaryotic cells.

ACKNOWLEDGMENT

The authors thank Dr. David M. Noll for helpful discussions.

REFERENCES

1. Colvin, M. (1982) *The Alkylating Agents*, W. B. Saunders Co., Philadelphia.
2. Thomas, C. B., Osieka, R., and Kohn, K. W. (1978) DNA cross-linking by *in vivo* treatment with 1-(2-chloroethyl)-3-(4-methylcyclohexyl)-1-nitrosourea of sensitive and resistant human colon carcinoma xenografts in nude mice, *Cancer Res. 38*, 2448−2453.
3. Erickson, L. C., Bradley, M. O., Ducore, J. M., Ewig, R. A. G., and Kohn, K. W. (1980) DNA crosslinking and cytotoxicity in normal and transformed human cells treated with antitumor nitrosoureas, *Proc. Natl. Acad. Sci. U.S.A. 77*, 467−471.
4. Garcia, S. T., McQuillan, A., and Panasci, L. (1988) Correlation between the cytotoxicity of melphalan and DNA cross-links as detected by the ethidium bromide fluorescence assay in the F_1 variant of B_{16} melanoma cells, *Biochem. Pharmacol. 37*, 3189−3192.
5. Grueneberg, D. A., Ojwang, J. O., Benasutti, M., Hartman, S., and Loechler, E. L. (1991) Construction of a human shuttle vector containing a single nitrogen mustard interstrand, DNA-DNA cross-link at a unique plasmid location, *Cancer Res. 51*, 2268−72.
6. Ojwang, J. O., Grueneberg, D. A., and Loechler, E. L. (1989) Synthesis of a duplex oligonucleotide containing a nitrogen mustard interstrand DNA-DNA cross-link, *Cancer Res. 49*, 6529−37.
7. Rink, S. M., Solomon, M. S., Taylor, M. J., Rajur, S. B., McLaughlin, L. W., and Hopkins, P. B. (1993) Covalent structure of a nitrogen mustard-induced DNA interstrand cross-link - an N7-to-N7 linkage of deoxyguanosine residues at the duplex sequence 5′-d(GNC), *J. Am. Chem. Soc. 115*, 2551−2557.
8. Rink, S. M., and Hopkins, P. B. (1995) A mechlorethamine-induced DNA interstrand cross-link bends duplex DNA, *Biochemistry 34*, 1439−1445.
9. Noll, D. M., Noronha, A. M., and Miller, P. S. (2001) Synthesis and characterization of DNA duplexes containing an N^4C-Ethyl-N^4C interstrand cross-link, *J. Am. Chem. Soc. 123*, 3405−3411.
10. Noronha, A. M., Noll, D. M., and Miller, P. S. (2001) Syntheses of DNA duplexes containing a C−C interstrand cross-link, *Nucleosides Nucleotides 20*, 1303−1307.
11. Noronha, A. M., Noll, D. M., Wilds, C. J., and Miller, P. S. (2002) N^4C-Ethyl-N^4C Cross-linked DNA: Synthesis and characterization of duplexes with interstrand cross-links of different orientations, *Biochemistry 41*, 760−771.
12. Puglisi, J. D., and Tinoco, I., Jr. (1989) Absorbance melting curves of RNA., *Methods Enzymol. 180*, 304−325.
13. Koo, H.-S., and Crothers, D. M. (1988) Calibration of DNA curvature and a unified description of sequence-directed bending, *Proc. Natl. Acad. Sci. U.S.A. 85*, 1763−1767.
14. Braich, R. S., and Damha, M. J. (1997) Regiospecific solid-phase synthesis of branched oligonucleotides. Effect of vicinal 2′,5′-(or 2′,3′-) and 3′,5′-phosphodiester linkages on the formation of hairpin DNA, *Bioconjugate Chem. 8*, 370−377.
15. Kierzek, R., Kopp, D. W., Edmonds, M., and Caruthers, M. H. (1986) Chemical synthesis of branched RNA, *Nucleic Acids Res. 14*, 4751−4764.
16. Scaringe, S. A., Wincott, F. E., and Caruthers, M. H. (1998) Novel RNA synthesis method using 5′−O-silyl-2′-O-orthoester protecting groups, *J. Am. Chem. Soc. 120*, 11820−11821.
17. Bellon, S. F., and Lippard, S. J. (1990) Bending studies of DNA site-specifically modified by cisplatin, *trans*-diamminedichloroplatinum(II) and *cis*-[Pt(NH_3)2(N^3-cytosine)Cl]+, *Biophys. Chem. 35*, 179−188.
18. Dong, Q., Barsky, D., Colvin, M. E., Melius, D. F., Ludeman, S. M., Moravek, J. F., Colvin, O. M., Bigner, D. D., Modrich, P., and Friedman, H. S. (1995) A structural basis for a phosphoramide mustard-induced DNA interstrand cross-link at 5′-d(GAC), *Proc. Natl. Acad. Sci. U.S.A. 92*, 12170−12174.
19. Gray, D. M., Ratliff, R. I., and Vaughan, M. R. (1992) Circular dichroism spectroscopy of DNA, *Methods Enzymol. 211*, 389−405.
20. Osborne, S. E., Vo1lker, J., Stevens, S. Y., Breslauer, K. J., and Glick, G. D. (1996) Design, synthesis, and analysis of disulfide cross-linked DNA duplexes, *J. Am. Chem. Soc. 118*, 11993−12003.
21. Harrington, R. E. (1993) Studies of DNA bending and flexibility using gel electrophoresis, *Electrophoresis 14*, 732−746.
22. Nadeau, J. G., and Crothers, D. M. (1989) Structural basis for DNA bending, *Proc. Natl. Acad. Sci. U.S.A. 86*, 2622−2626.
23. Koo, H. S., Drak, J., Rice, J. A., and Crothers, D. M. (1990) Determination of the extent of DNA bending by an adenine-thymine tract, *Biochemistry 29*, 4227−4234.
24. Brabec, V., Sip, M., and Leng, M. (1993) DNA conformational change produced by the site-specific interstrand cross-link of *trans*-diamminedichloroplatinum(II), *Biochemistry 32*, 11676−11681.
25. Paquet, F., Boudvillain, M., Lancelot, G., and Leng, M. (1999) NMR solution structure of a DNA dodecamer containing a transplatin interstrand GN7-CN3 cross-link., *Nucleic Acids Res. 27*, 4261−4268.
26. Sip, M., Schwartz, A., Vovelle, F., Ptak, M., and Leng, M. (1992) Distortions induced in DNA by *cis*-platinum interstrand adducts, *Biochemistry 31*, 2508−2513.
27. Coste, F., Malinge, J. M., Serre, L., Shepard, W., Roth, M., Leng, M., and Zelwer, C. (1999) Crystal structure of a double-stranded DNA containing a cisplatin interstrand cross-link at 1.63 A resolution: hydration of a platinated site., *Nucleic Acids Res. 27*, 1837−1846.
28. Kowalczyk, A., Carmical, J. R., Zou, Y. Van Houten, B., Lloyd, R. S., Harris, C. M. and Harris, T. M. (2002) Intrastrand DNA cross-links as tools for studying DNA replication and repair: Two-, three-, and four-carbon tethers between the N^2 positions of adjacent guanines, *Biochemistry 41*, 3109−3118.
29. Rink, S. M., Lipman, R., Alley, S. C., Hopkins, P. B., and Tomasz, M. (1996) Bending of DNA by the mitomycin C-induced, GpG intrastrand cross-link, *Chem. Res. Toxicol. 9*, 382−389.
30. Dooley, P. A., Tsarouhtsis, D., Korbel, G. A., Nechev, L. V., Shearer, J., Zegar, I. S., Harris, C. M., Stone, M. P., and Harris, T. M. (2001) Structural studies of an oligodeoxynucleotide containing a trimethylene interstrand cross-link in a 5′-(CpG) motif: Model of a malondialdehyde cross-link, *J. Am. Chem. Soc. 123*, 1730−1739.

BI025671J